Photoacoustics 14 (2019) 19–30

Contents lists available at ScienceDirect

Photoacoustics

journal homepage: www.elsevier.com/locate/pacs

Cardiovascular optoacoustics: From mice to men – A review

Angelos Karlas[a,b,c,d], Nikolina-Alexia Fasoula[a,b], Korbinian Paul-Yuan[a,b], Josefine Reber[b], Michael Kallmayer[c,d], Dmitry Bozhko[a,b], Markus Seeger[a,b], Hans-Henning Eckstein[c,d], Moritz Wildgruber[e,f], Vasilis Ntziachristos[a,b,d,*]

[a] Chair of Biological Imaging, TranslaTUM, Technical University of Munich, Munich, Germany
[b] Institute of Biological and Medical Imaging, Helmholtz Zentrum München, Neuherberg, Germany
[c] Clinic for Vascular and Endovascular Surgery, University Hospital rechts der Isar, Munich, Germany
[d] German Center for Cardiovascular Research (DZHK), partner site Munich Heart Alliance, Munich, Germany
[e] Institute for Diagnostic and Interventional Radiology, University Hospital rechts der Isar, Munich, Germany
[f] Institute for Clinical Radiology, University Hospital Muenster, Muenster, Germany

ARTICLE INFO

Keywords:
Non-invasive imaging
Cardiovascular disease
Photoacoustics
MSOT
Clinical translation

ABSTRACT

Imaging has become an indispensable tool in the research and clinical management of cardiovascular disease (CVD). An array of imaging technologies is considered for CVD diagnostics and therapeutic assessment, ranging from ultrasonography, X-ray computed tomography and magnetic resonance imaging to nuclear and optical imaging methods. Each method has different operational characteristics and assesses different aspects of CVD pathophysiology; nevertheless, more information is desirable for achieving a comprehensive view of the disease. Optoacoustic (photoacoustic) imaging is an emerging modality promising to offer novel information on CVD parameters by allowing high-resolution imaging of optical contrast several centimeters deep inside tissue. Implemented with illumination at several wavelengths, multi-spectral optoacoustic tomography (MSOT) in particular, is sensitive to oxygenated and deoxygenated hemoglobin, water and lipids allowing imaging of the vasculature, tissue oxygen saturation and metabolic or inflammatory parameters. Progress with fast-tuning lasers, parallel detection and advanced image reconstruction and data-processing algorithms have recently transformed optoacoustics from a laboratory tool to a promising modality for small animal and clinical imaging. We review progress with optoacoustic CVD imaging, highlight the research and diagnostic potential and current applications and discuss the advantages, limitations and possibilities for integration into clinical routine.

1. Introduction

Cardiovascular disease (CVD) remains the most frequent cause of death. In efforts to effectively diagnose, manage and treat CVD, clinicians routinely utilize all major radiological imaging methods. Ultrasonography (US), the most commonly used modality in cardiovascular medicine, reveals morphological and functional information, which is useful for assessing the vascular wall or soft cardiac tissues, such as cardiac muscle and pericardium. Doppler US visualizes blood flow, and contrast-enhanced US (CEUS) uses dedicated contrast agents to provide indirect information on inflammation, ischemia, and angiogenesis [1,2]. Moreover, several other ultrasound-based techniques have been considered within the last decade for assessing different CVD features [3–5]. Chest X-ray, although of limited specificity and resolution, is still utilized to offer an inexpensive initial assessment of the cardiac silhouette and the large vessels of the chest. X-ray catheter angiography is the gold standard for investigating occlusive atherosclerotic lesions and guiding interventions [6,7]. Computed tomography angiography (CTA) is considered a non-invasive alternative to catheter angiography but at the expense of lower temporal resolution and motion-related artifacts [8]. Magnetic resonance imaging (MRI) is also a widely spread modality for both cardiac and vascular imaging due to its high resolution and use of safe, non-ionizing radiation. While X-ray and MRI techniques offer morphological and possibly functional information, they are not suitable for imaging specific pathophysiological processes at the molecular level. For this reason, nuclear medicine techniques, such as positron emission tomography (PET) and single-proton emission computed tomography (SPECT) are commonly used as on their own or in combination with CT and MRI for imaging metabolic or inflammatory processes, thus complementing morphological readouts with molecular information [9].

There is an ongoing debate on the appropriate use of available

* Corresponding author at: Chair of Biological Imaging, TranslaTUM, Technical University of Munich, Munich, Germany.
E-mail address: v.ntziachristos@tum.de (V. Ntziachristos).

https://doi.org/10.1016/j.pacs.2019.03.001
Received 14 March 2019; Accepted 18 March 2019
Available online 29 March 2019

imaging techniques assessing CVD. For example, imaging of the carotid plaque ulceration, a significant risk factor for stroke, can be done using various techniques (e.g. US, CEUS, CT, MRI), which have different diagnostic accuracies [10]. Likewise, it remains unclear what method to employ in valvular heart disease, such as valvular regurgitation, whereby both US and MRI may provide valuable information and drive clinical decisions [11,12]. In addition, current imaging technologies do not provide adequate information on patient selection for specific treatments. For example, carotid endarterectomy currently has to be performed in 21 patients (with moderate stenosis) in order to protect 1 patient from stroke, based on number-needed-to-treat analysis [13]. This means that the clear majority of patients undergoing this surgical procedure derive no clinical benefit. Imaging methods should be optimized to provide quantitative and biological meaningful biomarkers that align patients with treatments likely to benefit them.

While non-invasive clinical diagnostics currently rely on the abovementioned techniques, invasive techniques based on ultrasound or optical imaging have been also considered for CVD applications. Intravascular ultrasound (IVUS) provides relatively low contrast and resolution but remains the gold standard for vascular wall imaging due to its ability to image the full thickness of the arterial wall, even in the presence of large atherosclerotic plaques [14]. In addition, stent-based vascular interventions make frequent use of high-resolution optical coherence tomography (OCT) for intraprocedural navigation and treatment guidance, despite its limited ability to penetrate walls [15]. Morphological images of both IVUS and OCT may be further enhanced with molecular information on disease pathophysiology (e.g. atherosclerosis, stent thrombosis) by integrating additional optical technologies into the same catheter tip. For instance, near-infrared fluorescence (NIRF) and near-infrared spectroscopy (NIRS) have been widely used to image atherosclerotic plaques *in vivo* [16–18]. However, despite the informative contrast offered by interventional optical methods, non-invasive applications of optical methods are limited by the strong light scattering in tissue, which limits sensitivity and accurate visualization. For this reason, optical microscopy and tomography, such as fluorescence molecular tomography (FMT) or diffuse optical tomography (DOT), have been mostly considered for CVD research in mice or using invasive procedures [19–22].

Recently, optoacoustic imaging is widely considered as an optical imaging technique that is insensitive to photon scattering by tissue and therefore can yield high-resolution optical images through several millimeters to centimeters of tissue. The optoacoustic method, also termed photoacoustic in analogy to “photonic” imaging, detects ultrasound waves emitted through thermoelastic expansion of tissue moieties that absorb light of transient energy (Fig. 1a). According to the basic optoacoustic wave equation (Eq. 1), the optoacoustic wave pressure P depends on: the speed of sound ν_{ac} in a specific tissue; the volumetric thermal expansion coefficient β, which equals $(1/V)(\partial V/\partial T)$, where V is the volume and ∂V the volume change due to temperature change ∂T; and the specific heat capacity at constant pressure C_p, which refers to the thermal energy needed to change the local temperature by ∂T:

$$\left(\frac{1}{\nu_{ac}}\frac{\partial^2}{\partial t^2} - \nabla^2\right)P = \frac{\beta}{C_p}\frac{\partial}{\partial t}(\alpha I(\alpha)) \quad (1)$$

whereby the $\alpha I(\alpha)$ denotes the absorption of light in tissue and α is the light absorption coefficient in cm^{-1}. By using ultrasound detection, optoacoustic imaging yields high-resolution optical images that are insensitive to photon scattering and rather obey the laws of ultrasound image formation, i.e. the image resolution depends on ultrasonic diffraction and not photon scattering. The technique was first introduced in the 1970’s [23–25] but high-performing imaging systems appropriate for disseminated application are only now emerging, based on the evolution of fast lasers and high-performance methods for detection and data analysis [26–28]. These systems have now allowed first clinical studies in imaging cancer [29–31] and inflammation [32,33].

Optoacoustic imaging operates in portable ways that resemble US and allows integration into a hybrid mode together with ultrasound imaging, since both techniques can share a common ultrasound detector. Advantageously, the technique offers novel contrast not available to other radiology methods, by resolving optical absorption within tissues and being sensitive to hemoglobin. The technique can also sense water, lipids and melanin, which are the major endogenous tissue absorbers of light. By utilizing illumination at multiple wavelengths, multi-spectral optoacoustic tomography (MSOT) can differentiate chromophores, separating oxygenated from deoxygenated hemoglobin and offering images of blood oxygen saturation distribution in tissue or of lipid and water distributions without the need for exogenous contrast agents. Moreover, MSOT can achieve even greater molecular specificity through the use of exogenously administered agents and probes [34]. Although MSOT has limitations, including low penetration depth and highly complex data processing and analysis, its abilities may bring new opportunities for use in CVD applications, both in animal and human imaging. In the following we describe implementations of optoacoustic imaging in CVD, compare the technique performance to other modalities (Fig. 1b), explain advantages and limitations and review key applications that showcase the potential of optoacoustics in cardiovascular imaging tool.

In principle, optoacoustics can visualize any molecule that absorbs light at the illumination wavelength and preferentially emits the absorbed energy as acoustic waves rather than light (e.g. fluorescence). Using spectral differentiation, optoacoustics / MSOT can simultaneously resolve multiple chromophores. Chromophores can be endogenous, such as hemoglobins, myoglobins, lipids, collagen, and water; exogenous, such as gold-carrying nanoparticles, absorbing dyes and fluorescent agents such as indocyanine green; or genetically expressed fluorescent chromophores such as green fluorescence protein, lacZ, and violacein [35–38] (Fig. 2). The particular chromophores detected determine which cardiovascular processes can be monitored. For example, detection of hemoglobin provides insights into tissue oxygenation, vascularization and vascular dynamics whereby detecting lipids may provide insights into plaque composition.

2. Optoacoustic imaging based on endogenous chromophores

Oxygenated (HbO_2) and deoxygenated (Hb) hemoglobin are abundant in blood and have distinct optical spectra (Fig. 2a) which can be resolved by optoacoustic imaging. The ability of optoacoustics to detect hemoglobin and differentiate its oxygenation states allows direct imaging of blood vessels and quantification of soft tissue perfusion, oxygenation [27] or hemoglobin concentration [39]. This allows assessment of circulatory efficiency relative to local oxygen demand and gas exchange.

Optoacoustic imaging of vasculature has been considered for evaluating vascular malformations [40], functional assessment of dialysis fistulas, precise navigation during percutaneous cannulation procedures [41] and overall could contribute to non-invasive monitoring of critically ill patients experiencing rapid blood loss during surgical operations or trauma. The method has been further employed to image tissue perfusion and oxygenation in muscle affected by ischemic peripheral arterial disease or heart failure [42,43] and also detect deoxy- and oxy-myoglobin, providing insights into oxygen storage [44,45].

The ability of optoacoustics to detect lipids based on their spectral properties (absorption peak at 930 nm; Fig.2a) yield additional capacities for characterizing and monitoring atherosclerotic lesions [46]. MSOT has already been used to image subcutaneous adipose tissue in humans non-invasively [47], and further technological improvements could lead to the non-invasive detection of lipid-rich plaques, intraplaque hemorrhage, and perivascular fat of peripheral arteries *in vivo*, with significant implications for metabolic and CVD research. Moreover, by performing imaging at the characteristic light absorption

a

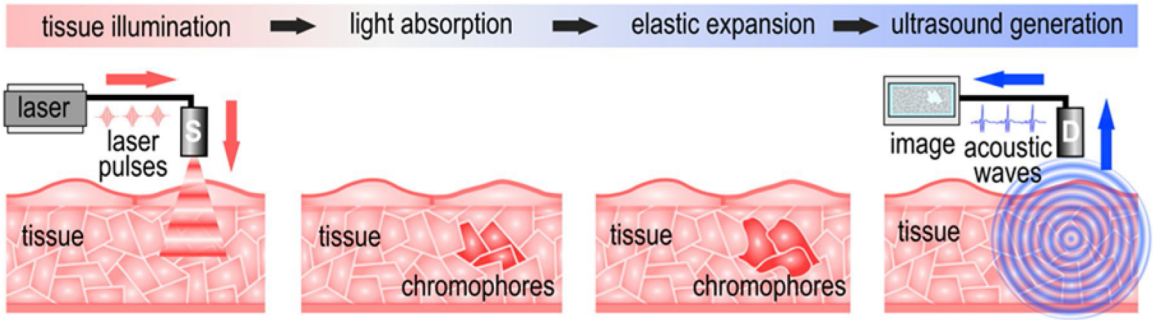

b

● Excellent ● Average ● Poor	Imaging performance					Information provided					Safety and usability					
	Penetration depth	Resolution vs. depth	Contrast	Sensitivity	Specificity	Morphological	Functional	Molecular	Dynamic or real-time	Multiscale	Non-ionizing radiation	Risks and side effects	Scanning time	Portability	Ease of use	Patient convenience
Optoacoustic	●	●	●	●	●	●	●	●	●	●	●	●	●	●	●	●
Optical	●	●	●	●	●	●	●	●	●	●	●	●	●	●	●	●
Ultrasound	●	●	●	●	●	●	●	●	●	●	●	●	●	●	●	●
X-ray	●	●	●	●	●	●	●	●	●	●	●	●	●	●	●	●
CT	●	●	●	●	●	●	●	●	●	●	●	●	●	●	●	●
MRI	●	●	●	●	●	●	●	●	●	●	●	●	●	●	●	●
PET	●	●	●	●	●	●	●	●	●	●	●	●	●	●	●	●
SPECT	●	●	●	●	●	●	●	●	●	●	●	●	●	●	●	●

Fig. 1. Optoacoustic imaging. (a) The optoacoustic phenomenon. Chromophores may be endogenous (e.g. hemoglobin, Fig. 2a) or exogenous (e.g. gold nanoparticles, Fig. 2b), (b) Comparison of optoacoustic and other clinical imaging modalities. Dot colors indicate relative performance in preclinical and, where known, clinical settings: green, excellent performance; yellow, average performance; red, poor performance. *Molecular,* ability to detect and quantify process-specific molecules within the tissue of interest. *Multiscale,* ability to exploit the same contrast mechanism to image at all levels of organization (e.g. organ, tissue, cell, molecule). S: Illumination source, D: Ultrasound detector, CT: computed tomography, MRI: magnetic resonance imaging, PET: positron emission tomography, SPECT: single proton emission computed tomography.

NIR peak of water at 970 nm (Fig. 2a), optoacoustic imaging is well suited to detect the water distribution in tissues.

Optoacoustics may also be useful in exploiting contrast from collagen, one of the main components of connective tissue, which shapes and mechanically supports other tissues and internal organs [48,49]. Preliminary capability to differentiate collagen from lipids has been shown in biological phantoms [48,50], suggesting also applications in characterizing changes in the collagenous tissue of the arterial wall in atherosclerotic disease [51]. Imaging collagen could contribute to assessing plaque destabilization, a parameter known to increase risk of acute cardiovascular events, such as myocardial infarction and stroke.

3. Optoacoustic imaging based on exogenous and genetically expressed chromophores

An even broader range of molecules and biological processes can be accessed with the optoacoustic method using exogenous contrast agents (Fig. 2b) and, in particular, agents with a strong light absorption ability (absorption cross-section). Among these agents, indocyanine green (ICG) is the only clinically approved dye available for optoacoustic imaging, featuring strong light absorption and low fluorescence quantum yield at NIR wavelengths [52]. Intravenously administered, ICG binds within seconds to plasma proteins and stays in the vasculature for 3–4 min before being excreted via the biliary tract. Its concentration in human blood falls at a rate of about 18.5% per minute but its presence in vasculature may be detected even 20 min after administration [53,54]. ICG can be used to visualize perfusion and permeability, to outline functioning vasculature and as a nonspecific marker of inflammation, targeting lipid-loaded macrophages [55]. It accumulates in 6–7 min within soft tissues, but it needs approximately 90 min to target lipid-rich macrophages in human carotid plaques [56]. ICG shows a relatively low photostability [57], leading to decreased detectability over time. To promote bioavailability and distribution within target tissue, ICG can be incorporated into the bilayer of clinically

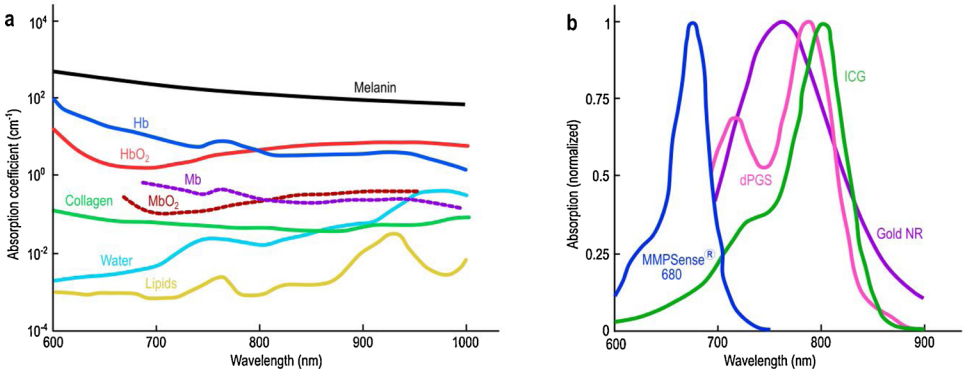

Fig. 2. Sources of optoacoustic contrast for cardiovascular applications. (a) Endogenous chromophores. (b) Exogenous chromophores used for optoacoustic studies of the cardiovascular system. HbO_2: Oxygenated hemoglobin, Hb: Deoxygenated hemoglobin, MbO_2: Oxygenated hemoglobin, Mb: Deoxygenated myoglobin, MMP: Matrix metalloproteinase, ICG: Indocyanine green, dPGS: Dendritic polyglycerol sulfates-NIR dye, Gold NR: Gold Nanorods.

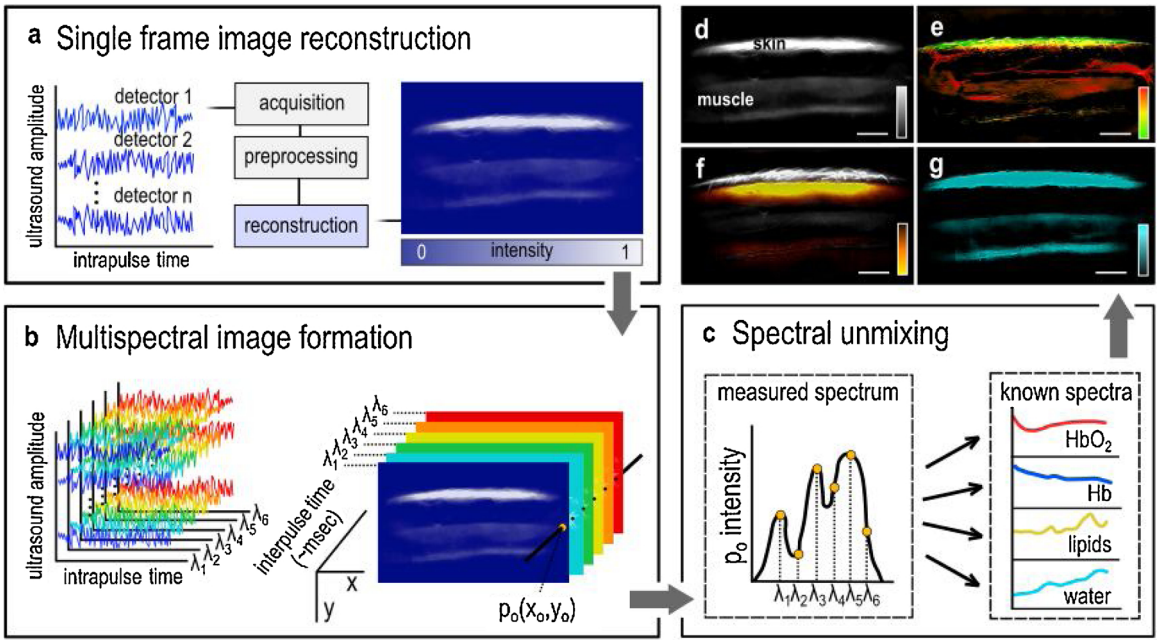

Fig. 3. Principle of operation of multispectral optoacoustic tomography (MSOT). (a) Upon absorption of a light pulse a single-wavelength frame is created by reconstructing the ultrasound signals recorded. (b) A stack of single-wavelength frames, defined by the number of wavelengths used to illuminate the tissue, constitute an optoacoustic multispectral image. (c) Each multispectral image is spectrally unmixed on a per-pixel basis using dedicated algorithms to calculate the contribution of each known chromophore (known spectrum) to each pixel (measured spectrum). HbO_2, oxyhemoglobin; Hb, deoxyhemoglobin; p_o, measured intensity of pixel (x_o,y_o) within the multispectral image. (d–g) MSOT imaging of the forearm of a healthy volunteer (Karlas et al., unpublished data), showing (d) a single-wavelength frame obtained at 800 nm (grayscale: optoacoustic intensity) and spectrally unmixed images of (e) hemoglobin content, (f) lipid content, and (g) water content. In panels (d)-(g), the grayscale and color scales indicate the relative concentration of the target chromophore. Scale bars: 5 mm.

approved PEGylated liposomes [36].

Targeted agents are also considered to demarcate specific functional or molecular profiles in tissues. Smart probes that use fluorescent dyes that are “turned on” upon cleavage by dedicated enzymes such as matrix metalloproteinases or cathepsins have been shown to have non-only a fluorescence but also an absorption modification upon activation and therefore they have been detected by MSOT in association with unstable plaque [58,59]. Another synthetic dye, dendritic polyglycerol sulfates-NIR (dPGS-NIR), has been used for *in vivo* imaging of intracardiac inflammation following iatrogenic myocardial infarction in a dedicated mouse model [60]. dPGS-NIR binds to P- and E-selectins, cell adhesion molecules involved in recruiting inflammatory cells to sites of inflammation in deep venous thrombosis, myocarditis, and atherosclerosis [61,62].

Various types of nanoparticles have been also developed for preclinical cardiovascular imaging, including liposomes [63], lipoprotein particles [64], and gold nanoparticles [65,66]. Gold nanoparticles, which have cytotoxic effects when stimulated by electromagnetic radiation, are particularly attractive for optoacoustic imaging [67]. They can be produced in a variety of sizes and shapes, including spheres, rods, shells, nanostars and triangles, which alters their biodistribution and absorbance spectra [35] in potentially interesting ways. Circulating gold nanorods allow MSOT-based dynamic imaging of the heart, aorta, and carotid arteries of mice [68]. Some calcium sensors, such as metallochromic compounds, have been also used in optoacoustic imaging, [69,70]. Nevertheless, issues with photo-stability may compromise longitudinal imaging using gold particles.

Genetically expressed optoacoustic markers also offer unique advantages for biomedical research as they can be very specific of desired cellular processes. Several genetic reporters have been used for preclinical optoacoustic imaging so far, including bacteriophytochrome-based near-infrared fluorescent protein (iRFP) [71], enhanced green fluorescent protein (eGFP) [72], tyrosinase/melanin [73], and violacein [37]. A reversibly activatable photoresponsive bacterial phytochrome (BphP1) with enhanced properties has recently been presented. It can undergo reversible photoconversion upon illumination at a specific wavelength [74]. It may be possible to engineer cardiac fibers to express BphP1 and thereby facilitate direct imaging of cardiac muscle [74]. The genetically expressed calcium indicator GCaMP5G, a fluorescent voltage sensor used so far mainly in fluorescence neuroimaging [75,76], may be useful for tracking cardiac tissue excitation events.

Future work should seek to capitalize on promising optoacoustic chromophores closer to the clinic as well as develop new chromophores for optoacoustics. As more exogenous probes receive clinical approval, the versatility of optoacoustics can be brought to bear on a broader array of cardiovascular disease processes.

4. Optoacoustic systems and techniques

Modern optoacoustic systems developed for non-invasive imaging are tailored to specific applications and can be categorized based on different criteria. A common classification is according to the penetration depth (δ) and/or spatial resolution ($\Delta\ell$) achieved. Generally, systems may be categorized as microscopic ($\delta < 1$ mm, $\Delta\ell \approx$ few μm), mesoscopic (1 mm $< \delta <$ 5–10 mm, $\Delta\ell \approx$ few-tens μm) and macroscopic ($\delta >$ 5–10 mm and $\Delta\ell \approx$ tens-hundreds μm) [77]. Optoacoustic implementations can be also monochromatic, when illuminating at a single wavelength, or multispectral, when illuminating at multiple wavelengths. Imaging can be performed in two modes: scanning of a single detector over the field of view (FOV), or acquisition of ultrasound signals in parallel with multi-element arrays. Systems using ultrasound element arrays can achieve video rate imaging, appropriate for capturing the highly dynamic character of the cardiovascular system. Such implementations can provide information on cardiovascular kinetics and tissue hemodynamics and metabolism *in vivo* [78,79]. Although the geometry and characteristics of these detectors may have different geometrical and bandwidth specifications compared to detectors employed in ultrasonography [80], the overall central frequency employed

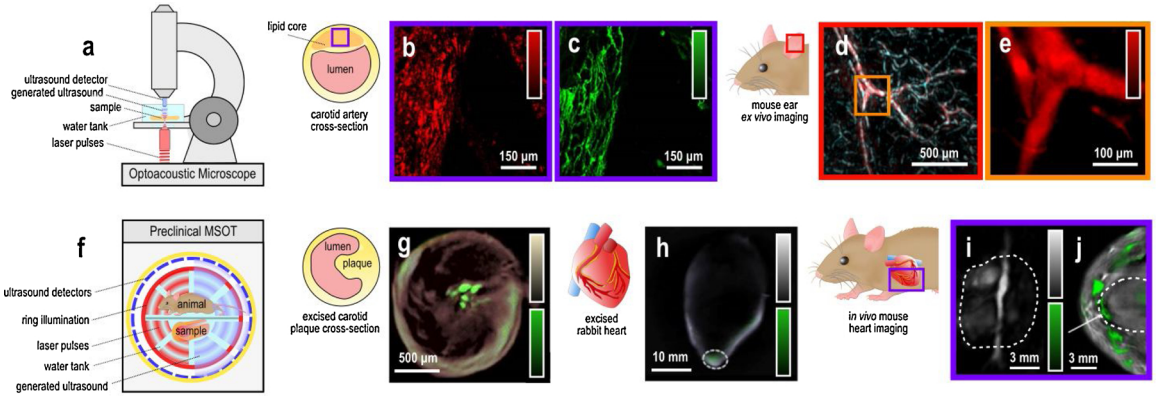

Fig. 4. Cardiovascular applications of preclinical optoacoustic imaging. (a–e) Optoacoustic microscopy of tissue samples. (a) Schematic illustration of Optoacoustic microscopy. (b) Optoacoustic signal over the lipid core of an excised human carotid atheroma depicting the distribution of red blood cells (red color scale). Reprinted with permission from [101]. (c) Second harmonic generation imaging of the same region as in panel (b) depicting the distribution of the collagen network within lipids (green color scale) in the core of the plaque. The loss of normal collagen bundle structure in panel (c) is associated with red blood cell accumulation in panel (b) [101]. (d) Microvascular network of a mouse ear imaged *ex vivo*. The area boxed in orange is shown as a close-up in panel (e). (e) Zoomed area corresponding to the orange frame of panel (d), depicting hemoglobin (red color scale) in a microvascular bifurcation. Reprinted with permission from [106]. (f–h) MSOT of excised tissues. (f) Schematic of preclinical MSOT for tissue and small animal imaging. (g) Image of an excised human carotid atheroma showing lipid distribution (beige color scale), overlaid with matrix metalloproteinase activity visible as MMPSense® 680 activation (green color scale). Reprinted with permission from [59]. (h) Image of an excised rabbit heart showing blood distribution (gray color scale) and stem cells labeled with Xenolight DiR® NIR-dye (green color scale). After labeling, the stem cells were injected into the myocardium (white dashed circle). Reprinted with permission from [122]. (i–j) MSOT of the heart of a small animal *in vivo,* obtained using a hand-held system equipped with a spherical ultrasound array. Images show the distribution of blood (gray color scale) and of selectin-targeting dPGS-NIR dye (green color scale) injected intravenously into the animal. (i) Image of the cardiac surface (white dashed line). The tubular structure in the foreground is one of the two superior venae cavae. Reprinted with permission from [123]. (j) Tomographic view of the chest showing the cardiac silhouette (white dashed line, white arrow). Reprinted with permission from [60].

matches that of ultrasound systems, i.e. it typically ranges between 1 – 25Mhz. Generally, macroscopic imaging is performed with frequencies in the few MHz whereby mesoscopic imaging is performed with frequencies in the few tens of MHz.

Video-rate Multispectral Optoacoustic Tomography (MSOT; Fig. 3) has been implemented in macroscopic imaging mode (˜3-7 MHz) and has been applied in various CVD applications in mice and humans. MSOT typically employs single-pulse-per-frame (SPPF) acquisition for minimizing motion artifacts that degrade spatial resolution and the accuracy of spectral unmixing. Typically operating in the “optical window” of 680–980 nm, MSOT achieves imaging depths of ˜2-5 cm depending on tissue type. As shown in Fig. 3b, different reconstructed images correspond to a different wavelength of illumination and display an intensity map of the absorption distribution at that wavelength. The stack of single-wavelength images forms a multispectral image that needs to be spectrally unmixed to reveal the contribution of each chromophore to each pixel. In this way, MSOT adds an additional (spectral) dimension to molecular imaging, creating a new paradigm for cardiovascular imaging because it allows simultaneous analysis of numerous relevant chromophores in the tissue, most of them endogenous. MSOT has already contributed to *in vivo* studies with animal CVD models [68], as well as to clinical vascular imaging, where it adds complementary information to the US examination of large vessels. Moreover MSOT has been shown superior to US when imaging smaller vessels down to 100 µm in diameter [81]. MSOT has also shown its usefulness in several clinical contexts outside the cardiovascular field, such as in cancer [82] and metabolic research [78] as well as in imaging the brain [83] or the gastrointestinal tract [32,84].

Implemented at frequencies in the few tens of MHz, optoacoustic mesoscopy has been also considered for animal or human imaging using multi-detector arrays [85] or raster-scan imaging. A particular implementation termed raster-scan optoacoustic mesoscopy (RSOM) employs broadband transducers that bridge mesoscopic and microscopic resolutions by performing imaging in the 20–200 MHz ultrasound frequency range [86,87] and was shown to offer sub 10 µm axial resolutions at penetration depths of ˜ 1–2 mm. This high depth-to-resolution ratio makes optoacoustic mesoscopy an excellent tool for imaging the skin, an easily-accessible organ that also may be employed as a window to CVD parameters. In particular, diabetes and hypertension have been correlated with a decrease in the density of skin capillaries [88], and cutaneous microvascular rarefaction has been detected in patients with chest angina and angiographically subtle stenoses [89]. Thus, microvascular disturbances of the skin may serve as a biomarker of generalized cardiovascular disease [90], so optoacoustic assessment of the skin may provide complementary diagnostic information [87,90,91]. RSOM, in particular, can determine several parameters of cutaneous microvasculature, i.e. the diameter of single microvessels ranging from the smallest capillaries to the larger arterioles and venules, total blood volume (TBV) in skin compartments, as well as density and complexity of the microvascular network [87]. Current RSOM systems capture FOVs of up to 4 mm × 4 mm at penetration depths of ˜ 2 mm in less than a minute, offering a larger FOV than conventional optical microscopy. Motion-correction algorithms can reduce or eliminate artifacts that arise due to voluntary or involuntary motion of the patient (e.g. respiration) or vascular structures (e.g. arterial pulsation); if uncorrected, these artifacts can degrade image quality and narrow the range of potential clinical applications [92].

Miniaturization of optoacoustic sensors has enabled the development of intravascular optoacoustics as a novel tool for studying atherosclerotic plaques, the rupture of which is a major cause of heart attack and stroke. Plaques likely to rupture, termed vulnerable plaques, feature a thin fibrous cap (< 65 µm), a large underlying lipid-necrotic core occupying > 10% of the plaque area, and intraplaque hemorrhage, and they are infiltrated by inflammatory cells such as macrophages and lymphocytes [93]. In large, histology-based studies of coronary atherosclerosis, existing imaging modalities have proven to be quite limited in their ability to identify vulnerable plaques [94,95]. Intravascular optoacoustics may be useful for assessing plaque vulnerability given that it offers spatial resolution of ˜50 µm [96] and can detect lipids, hemoglobin and injected markers of plaque inflammation.

Finally, optoacoustic imaging can be also implemented in microscopy mode using either optical focusing (i.e. optical resolution optoacoustic microscopy; OROM) or ultrasound detectors preferably in the 100’s of MHz, although systems with reduced resolution are also

implemented in lower frequencies [97]. Optoacoustic microscopy has also been employed in interrogations of cardiovascular features, particularly ex-vivo in tissue samples, as discussed in the following.

5. Preclinical applications of optoacoustics

5.1. Ex vivo optoacoustic imaging of cardiovascular tissue samples

Optoacoustic microscopy (Fig. 4a) has visualized the three-dimensional arrangement of the fibers in excised mouse cardiac muscle that have diameters of 10–25 μm and that are located in the ventricular myocardium with resolution < 1 μm [45]. The architecture of cardiac myocytes governs the electromechanical phenomena taking place during cardiac contraction and thus the pumping efficiency of the heart [98]. The main source of optoacoustic contrast in cardiac tissue is myoglobin [45], which has higher affinity for oxygen than hemoglobin does and which is particularly abundant in muscle fibers that must undergo periodic contractile activity for prolonged periods, such as cardiac fibers [99]. Furthermore, optoacoustic microscopy has been recently used to image the developing heart in the embryonic zebrafish [100], demonstrating potential in imaging myocardial fibers in animal models *ex vivo*. This ability introduces a new way for studying the mechanisms driving embryonic development of the heart or the processes leading to fiber disorganization in interstitial cardiac fibrosis, cardiomyopathies, and cardiac remodeling due to hypertension or myocardial infarction.

Optoacoustic microscopy becomes particularly powerful for cardiovascular research when it is combined with optical microscopy. An excised human carotid atheroma was imaged in a label-free mode using a hybrid microscope that combines optoacoustic microscopy, second and third harmonic generation microscopy, and two-photon fluorescence microscopy (Fig. 4b and 4c) [101,102]. The system yield spatial resolution of ˜ 1 μm for all embedded modalities and a penetration depth of ˜ 300 μm. Optoacoustic microscopy enabled accurate visualization of intraplaque hemoglobin offering the potential to image hemorrhage and angiogenesis, two critical factors of plaque vulnerability [103]. The combination of optoacoustics with other optical microcopy techniques yielded multimodal images that revealed direct interactions between red blood cells (optoacoustic microscopy), collagen (second harmonic generation, SHG) and elastin (two-photon excitation fluorescence, TPEF) within three parts of the plaque that are of major biological interest: the shoulder, cap, and lipid core. Collagen and elastin are two crucial components of the plaque, and their degradation increases risk of rupture and clinical events [104,105]. A great advantage of hybrid optoacoustic microscopy is that it employs the same illumination path with the other optical microscopy techniques, such as SHG and TPEF, enabling accurate co-registration and seamless multi-modal integration.

Optoacoustic imaging of microvessels (< 150–200 μm in diameter) can be used to acquire highly detailed planar images of the microvasculature, extract volumetric structural information as well as metrics for quantifying its complexity. Due to ease of access, the mouse ear offers an ideal model for optoacoustic microvascular imaging both *ex vivo* and *in vivo* (Fig. 4d and e) [106]. The mouse ear has been used as a model of angiogenesis, a process involved in diseases such as ischemia and atherosclerosis [107–109]. Revealing tissue microvascular architecture is of great interest not only for tracking the formation of new microvessels in samples such as atheromas but also for investigating the microvascular rarefaction in diseases such as diabetes and hypertension [110,111]. Of interest is the ability to combine static microvascular images with functional data, such as HbO_2, Hb, TBV, and sO_2 to enhance our understanding of physiology and pathophysiology.

Apart from optoacoustic microscopy, excised cardiovascular tissue samples have been examined by MSOT (Fig. 4f), at resolutions in the 100–300 micron range [112]. Macroscopic MSOT was used to image matrix-metalloproteinase (MMP) activity, an indicator of plaque inflammation and instability, in human carotid plaques *ex vivo* (Fig. 4g) [59]. Surgically excised plaques were incubated with a marker activatable by matrix metalloproteinases and imaged with a pre-clinical custom-made MSOT setup. The technique resolved MMP activity over the whole thickness of the plaque tissue, demonstrating potential for monitoring a significant component of plaque rupture pathophysiology. Early detection of vulnerable plaques and prediction of their rupture is the “holy grail” of cardiovascular medicine. Apart from the presence of inflammatory activity, plaque stability is also regulated by local biomechanical forces [113]. Optoacoustics has been already used to extract biomechanical and structural features of atherosclerotic plaques *ex vivo*. Optoacoustic signals carry information on plaque tissue viscoelasticity [114], which refers to the strain-stress response of plaque tissue to periodic loading due to blood pressure and flow fluctuations over consecutive cardiac cycles. This viscoelasticity can affect risk of plaque rupture [115]. Therefore, the optoacoustic method presents new possibilities for studying structural and molecular parameters of plaque in excised specimen. Imaging these features may be particularly useful for understanding atherosclerosis and guiding treatment. Morphological maps of endogenous chromophores—hemoglobin in intraplaque micro-neovessels and hemorrhage, lipids in atheromas, and collagen in fibrotic tissue—can be combined with molecular maps of chromophores involved in necrosis, inflammation, and intraplaque angiogenesis. This approach may substantially advance our understanding of how plaques destabilize and rupture, which can trigger acute events such as myocardial infarction and stroke.

5.2. In vivo optoacoustic imaging of small animals

Optoacoustic imaging has been employed to characterize structural and functional features of the micro- and macrovasculature *in-vivo*, including visualization of tissue perfusion and oxygenation in animal models. Disturbances of tissue hemodynamics and arterial stiffness associate with an increased risk for stroke and coronary artery disease [116,117]. Optoacoustic microscopy has been used to measure the pulse wave velocity (PWV) [118], an index of arterial stiffness, in peripheral murine vessels. This work involved a custom-made electrocardiographic gating system to synchronize the optoacoustic blood flow speed measurements with the cardiac pulse. The system gives a temporal resolution of 0.65 ms for blood flow speed measurements providing the potential to measure PWVs up to 1.6 m/s. As a reference, mean PWV is approximately 1.9 m/s in the aorta of healthy adult mice [119] and approximately 6.2 m/s in the carotid-femoral artery of healthy young adults [120].

MSOT using gold nanoparticles has also shown ability to track vascular and cardiac hemodynamics in mice in real time [68]. Generally, the use of single-pulse-per-frame (SPPF) acquisition minimizes motion artifacts and can capture different phases of the cardiac cycle (e.g systole vs. diastole). Nevertheless, advanced deblurring techniques have been shown to further improve image quality of dynamic measurements [121]. Information on the left ventricular wall throughout the cardiac cycle can be extracted in a short-axis tomographic view using systems equipped with linear concave ultrasound arrays [121]. Moreover, MSOT has been employed to image myocardial infarction in a dedicated mouse model (Fig. 4j) [60]. Myocardial infarction, the necrotic result of sustained ischemia and anoxia, compromises the efficiency of cardiac contraction and is followed by complex inflammatory and remodeling processes. Mice imaged 48 h after infarction and injection of dPGS-NIR dye targeting P- and L-selectins demonstrated imaging of inflammation occurring in the myocardium. Optoacoustic imaging has also been used for longitudinal imaging of structural and biological changes following pharmacological, surgical and regenerative interventions, or following irreversible myocardial damage, for example by tracking intramyocardially-injected stem cells (labeled with 5–10 μg of Xenolight DiR® NIR-dye) in rabbits (Fig. 4h) [122].

Optoacoustic implementations using ultrasound arrays with elements arranged around a spherical surface have also been considered and have shown great capability for monitoring mouse cardiac dynamics in real-time by extracting information on the synchronization between atria and ventricles, as well as for monitoring the real-time perfusion of injected fluorescence agents (ICG) within the heart [123]. However, this approach provides limited penetration depth down to only 10 mm, preventing full-depth tomographic visualization of the heart, even in small animal models.

Blood perfusion and oxygen saturation of soft tissues such as muscles reflect not only the efficiency of the cardiovascular system to deliver nutrients but also the viability and metabolic status of the tissue. Recently, a novel nonlinear spectral unmixing technique for preclinical MSOT data was presented that allows quantification of the levels of perfusion and oxygen saturation deep in tissues *in vivo* [27]. Parenchymal oxygen saturation in murine muscular tissue was estimated with 3–8 times better accuracy than traditional linear unmixing techniques for penetration deeper than 5 mm. The novel method enhanced accuracy by correcting for "spectral coloring", which refers to the depth-dependent deviation of the measured absorption spectrum of a chromophore from the expected spectrum. This deviation arises because different tissues absorb and scatter light differently, so the light energy delivered to a chromophore depends on the tissues lying between the illuminated surface and the chromophore. Therefore, the deviation depends on depth. It also depends on wavelength because different tissues absorb and scatter different wavelengths to different extents. It is anticipated that the development of novel spectral unmixing techniques to precisely measure hemoglobin gradients and functional status of deep tissues will have translational potential in several CVD disorders (e.g. critical limb ischemia), where early diagnosis may allow interventions to reverse impaired soft tissue oxygenation and tissue loss.

6. Clinically-oriented cardiovascular optoacoustics

6.1. Non-invasive vascular imaging using MSOT

Various traditional technologies are currently used for imaging the vascular system in the clinical setting. Handheld US offers great flexibility because it can acquire real-time anatomical and blood flow (Doppler) data, but it cannot provide direct molecular information [11]. Nuclear imaging techniques like PET visualize ischemia and functional processes such as inflammation, yet with low spatial resolution (4–5 mm) and inevitable radiation exposure [124]. Despite the development of advanced CT systems that achieve high resolution in space ($<$ 1 mm) and time ($<$ 100 ms), the use of ionizing radiation remains a limiting factor [125]. Finally, MRI provides high-quality structural information with resolution that may be better than 1 mm and functional imaging with temporal resolution of 20–50 ms, giving insights into tissue perfusion, collagen, fat, and water content but with increased patient inconvenience and less flexibility than with handheld devices [11,125]. Several hybrid scanners, such as PET/CT and PET/MRI, have been introduced to overcome the main limitations of current standalone techniques and provide complementary structural, functional, and molecular data.

Optoacoustics provide information not generally available to the established radiological methods. MSOT systems have been developed as hybrid systems with ultrasonography and offer portable, user-friendly scanners for anatomical, functional and potentially molecular readings, collected in real-time. The technique has been already employed to image aspects of the vascular system in humans (Fig. 5a) [81,126], including the carotid artery. Overall, atherosclerotic disease is a major clinical problem, so there is an unmet need for non-invasive imaging of lipid-rich plaques, intraplaque hemorrhage or therapeutic agents against plaques and in-stent inflammation. Ultrasound imaging is currently the most frequently used clinical imaging modality to assess carotid atherosclerosis based on anatomical and possibly blood flow features. Unlike ultrasound, optoacoustics has the potential to characterize physiological and biochemical plaque parameters by characterizing lipid composition and presence of intraplaque haemorrhage. Therefore, hybrid application of optoacoustics and ultrasonography can improve the desease detection and assessment.

A custom-made hand-held optoacoustic imaging probe was able to image the common carotid artery and the jugular vein in a healthy volunteer with high optical contrast and resolution [127] (Fig. 5b). Nevertheless, the carotid artery is a challenging target for optoacoustic imaging. First, light attenuation reduces the signal strength at the carotid depths [128]. Moreover, spectral coloring, i.e. the depth dependent change of the apparent spectrum recorded by an optical method due to differential attenuation of different tissues [129] complicates the accuracy of spectral unmixing techniques. An additional limitation is that the bundles or sheets (fascia) of connective tissue between the layers of sternocleidomastoid and other muscle overlying the carotid act as an acoustic reflector that also weakens the optoacoustic signal before its detection. Therefore, technical developments are required for accurate carotid plaque optoacoustic visualization *in vivo*, in particular in terms of reconstruction and spectral unmixing improvements.

A less challenging application of optoacoustic imaging is the visualization of the foot dorsal artery and the posterior tibial artery, both of which are relevant to peripheral arterial disease. For these arteries, MSOT may be superior to conventional ultrasonography for visualizing vasculature at the meso- and micro-scales [81]. MSOT has been shown to resolve vessels of diameters $<$ than 100 μm in diameter, which are much smaller than the vessels typically resolved by clinical ultrasonography (˜ 1 mm). MSOT also shows high precision when measuring and tracking arterial dimensions and small vessels over time (Fig. 5c, d) [126]. This allows, for example, flow-mediated dilatation (FMD) tests of macrovascular endothelial function with high spatial and temporal resolution [126]. It may be possible to further improve traditional macrovascular FMD tests by combining microvascular, tissue-level and perhaps biological information (e.g. assays of nitric oxide or vascular inflammation markers). This may be a novel multiscale approach for testing endothelial function in the clinic.

Non-invasive monitoring of tissue hemodynamics and oxygenation is an additional imaging ability offered by optoacoustics and can be employed to assess tissue metabolism and viability *in vivo*. Imaging muscle hemodynamics (Fig. 5e) under different conditions offers valuable information within the fields of muscle physiology, oxygen kinetics and metabolism as well as vascular and metabolic diseases, such as peripheral arterial disease, diabetes, and heart failure. MSOT can detect and quantify these changes in real-time with high sensitivity deep in soft tissue, under conditions of high oxygen demand and consumption (e.g. exercise) or low blood and oxygen supply (e.g. arterial occlusion). An intensity-based approach has been already employed to track exercise-induced changes in muscle and skin perfusion and oxygenation over the femoral region of healthy volunteers [132]. Information on the fluctuations of HbO_2, Hb, and TBV was extracted by tracking the recorded intensities over a manually-segmented muscle region within the optoacoustic frames acquired after illumination at 850, 750 and 800 nm.

Advances in image analysis methods, including novel spectral unmixing techniques, will allow a more precise monitoring of muscle hemodynamics and oxygen kinetics by (1) directly estimating blood and oxygen saturation changes in soft tissues in a more physiological and intuitive manner that goes beyond preliminary intensity analysis, and (2) facilitating manual or automated segmentation of muscle based on additional information about blood and water content and lipid-water differentiation (Fig. 3d–g). Thus, by providing precise visualization of soft tissues, real-time monitoring of soft tissue hemodynamics, as well as direct macro- and microvascular imaging, MSOT (Fig. 5b–e) and RSOM (Fig. 5f) offer access to a novel multiscale and integrated approach to understanding physiological and pathophysiological

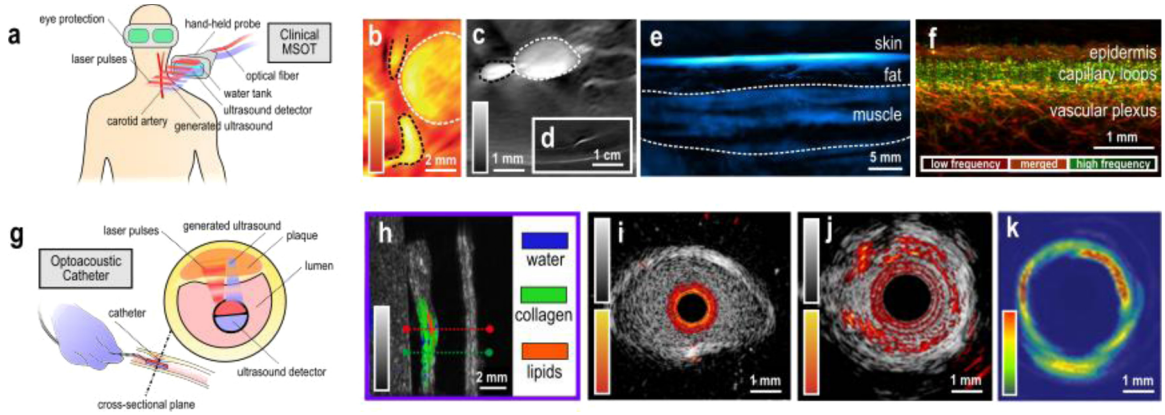

Fig. 5. Clinically-oriented cardiovascular optoacoustics. (a–f) Non-invasive applications. (a) Schematic representation of clinical carotid imaging using MSOT. (b) MSOT image of the carotid artery (white dashed line) and jugular vein (black dashed lines) of a healthy volunteer (yellow-orange color scale: optoacoustic intensity at 800 nm). Reprinted with permission from [26]. (c) MSOT image of the radial artery (white dashed line) and a vein (black dashed line) in the forearm of a healthy volunteer (gray color scale: light absorption at 800 nm). Reprinted with permission from [126]. (d) MSOT image of the same region as in panel (c), showing a small vessel with a diameter of ≈ 0.5 mm (Karlas et al. unpublished data). (e) MSOT image of the same region as in panel (c), showing the brachioradialis muscle (white dashed line) (blue color scale: light absorption at 800 nm which represents the TBV) (Karlas et al. unpublished data). (f) RSOM image showing the skin microvasculature of a healthy volunteer. Low-frequency components of the image, corresponding to larger microvessels, are shown on a red color scale; high-frequency components, corresponding to smaller microvessels, are shown on a green color scale. Merged low- and high-frequency components are shown on an orange color scale. Reprinted with permission from [87]. (g–k) Invasive (catheter-based) applications. (g) Schematic representation of intravascular optoacoustics. (h) *Ex vivo* optoacoustic imaging of a human carotid artery in a neck phantom, with ultrasound contrast shown on a gray color scale and optoacoustic contrast shown as blue, green or orange depending on tissue composition. Reprinted with permission from [48]. (i) Combined IVUS (gray color scale) and optoacoustic imaging (orange-red color scale) of an excised healthy rabbit aorta illuminated at 1720 nm through blood. Reprinted with permission from [130]. (j) Combined intravascular ultrasound (IVUS, gray color scale) and optoacoustic imaging (orange-red color scale) of an excised atheromatous rabbit aorta at 1720 nm through blood. Reprinted with permission from [130]. (k) Two-dimensional map of lipid distribution within the wall of a rabbit aorta *in vivo*. The red-green color scale shows relative lipid concentration. Reprinted with permission from [131].

processes under conditions such as exercise, peripheral ischemia and diabetes.

6.2. Intravascular optoacoustic imaging

The need to identify and characterize high-risk vulnerable plaques and visualize stents has led to the development of several standalone and multimodal intravascular imaging techniques [133]. The techniques currently qualified for everyday clinical use, IVUS and OCT, image wall morphology and stent configuration, but they do not provide functional information relevant for plaque tissue characterization or disease quantification [94,134]. To tackle this challenge, modern preclinical configurations employ optical molecular imaging technologies, such as NIRS [135], fluorescence life-time imaging (FLIM) [136], and especially NIRF imaging [16]. These techniques have been used to visualize processes such as plaque inflammation [137], protease activity [138], and oxidation of low-density lipoprotein [139], making them complementary to purely morphological IVUS and OCT. All these optical techniques, however, currently provide two-dimensional fluorescence maps of the inner surface of the vascular wall. They cannot effectively resolve the detected fluorescence signal and extract molecular information across the entire thickness of the atherosclerotic wall.

Intravascular optoacoustic imaging also commonly referred to as intravascular photoacoustic imaging (IVPA, Fig. 5g), may develop into an intravascular imaging modality able to conduct precise three-dimensional molecular profiling of atherosclerotic tissue. IVPA has the unique potential to combine volumetric three-dimensional information on plaque structure, composition, and biology by mapping the light absorption within plaque tissue at multiple wavelengths and resolving the spectral signatures of endogenous or exogenous light absorbers. The efficacy of IVPA relies on extracting depth information based on the time delay with which ultrasound signals arrive at the detector: longer delays correspond to deeper acoustic-emitting chromophores. It has been shown that an axial resolution of ˜ 50 µm can be achieved and maintained at distances up to 5 mm in tissue by employing high-frequency intravascular ultrasound detectors with a central frequency of 45 MHz [96].

IVPA was first used to differentiate among collagen, water and lipid content within the subendothelial layer of the vascular wall *ex vivo* by acquiring multispectral data at the near-infrared range of 1130–1250 nm in the absence of luminal blood (Fig. 5h) [48]. The presence of luminal blood around the imaging catheter leads to strong light absorption and scattering and thus to substantial signal loss. Nevertheless, accurate IVPA imaging can be conducted in the presence of luminal blood, as already demonstrated in dedicated vascular phantoms [140] and arteries *ex vivo* (Fig. 5i, j) [130]. However, to further eliminate the effect of light attenuation and scattering through blood, flushing with normal saline or the less light-absorbing heavy water (D_2O) may be also applied, analogously to purely optical techniques (OCT, NIRS, FLIM), which require flushing. Moreover, by recording the optoacoustic responses to illumination at multiple wavelengths, multispectral data can be acquired, and different plaque components can be differentiated. Thus, by illuminating at two wavelengths (1200 and 1700 nm), both absorption peaks of lipids can be used to identify lipid-rich plaques, as demonstrated in rabbit aortas *in vivo* (Fig. 5k) [131].

Several designs of IVPA catheters have been presented so far in efforts to provide the small size, high sensitivity and high speed required for imaging atherosclerosis in the clinic. The same ultrasound transducer already widely used for IVUS in the clinic has been applied to simultaneous IVUS and IVPA imaging, simplifying the final catheter design and keeping it < 1 mm for intravascular imaging [141]. All-optical implementation of optoacoustic imaging provides a promising alternative to commonly used piezoelectric elements, allowing miniaturization while retaining high sensitivity; such all-optical systems can be combined with simultaneous OCT imaging [142]. The spatial resolution of such systems is less than 50 µm down to depths of approximately 2.5 mm, based on phantom studies. The collinear alignment of the optical and optoacoustically-generated sound waves could increase the sensitivity of IVPA imaging in order to reach as deep as 6 mm [143]. However, such a deep-penetrating system would require a catheter diameter of 1.6 mm, which would prevent its use in

intracoronary procedures. Moreover, the mechanical rotation of the IVPA catheter as well as the relatively long data acquisition and processing times hinder real-time intravascular imaging. Novel designs for IVPA imaging at video-rates (25 frames per second) promise to make such systems useful in the clinic [144].

Thus, modern miniaturized multispectral catheter-based optoacoustic systems show potential for providing fast information about plaque stability, but their clinical implementation will be limited by the high cost of fast multispectral pulsed light sources and the low signal-to-noise ratio due to catheter sheath attenuation and the presence of blood. In any case, the invasive nature of intravascular techniques increases the risk of complications such as perforation, thrombosis, and infections, and it creates stress for clinicians and inconvenience for patients. In the long term, it may make more sense to focus on increasing the sensitivity and specificity of non-invasive clinical optoacoustic systems aimed at detecting and quantifying biomarkers of atherosclerotic disease.

7. Limitations and technical considerations

Optoacoustic technology may well be a useful tool for cardiovascular imaging, but it is not without its limitations. Recorded acoustic signals require complex processing and analysis to be reconstructed into precise images or to provide accurate spectral unmixing results. The complexity of all steps of image production necessitates the use of specialized algorithms that prolong processing.

Furthermore, the limited field of view and limited bandwidth detection of typical hand-held scanning probes introduces inaccuracies into image reconstruction, which distort the morphology of structures such as blood vessels and degrade data quality. Thus, precise clinical imaging remains challenging despite great advances in preclinical optoacoustic setups. The development of advanced optoacoustic image reconstruction methods is expected to eliminate image artifacts that decrease the signal-to-noise ratio and hinder data interpretation.

Spectral unmixing of multispectral data is conducted on a per-pixel basis, making unmixing results susceptible to motion-related artifacts. Such motion may involve the patient (e.g. breathing, heart beat or body motion) or the examiner (e.g. when the scanning probe moves relative to the imaged tissue).

Moreover, spectral unmixing is greatly influenced by spectral coloring: as light travels through tissue, it is absorbed and scattered to different extents depending on its wavelength. As a result, transmitted light reaches the depth of interest at different energy levels, and the measured spectrum of a specific absorber (e.g. HbO_2) may be quite different from the expected one, critically degrading the precision of spectral unmixing. Spectral coloring occurs in parallel with the attenuation of light fluence with depth, which decreases the penetration depth of optoacoustics. The sensitivity and spatial resolution of optoacoustic images also decrease with depth because of light scattering, making detailed imaging of highly perfused organs, such as the heart, skeletal muscle or liver, a great challenge. Novel methods are needed to compensate for wavelength-dependent fluence attenuation and spectral coloring to achieve optoacoustic imaging deeper in tissue with precise quantification of absorption.

The design and development of accurate algorithms to overcome these limitations require excellent understanding of optoacoustic theory and computational models. Although clinically-oriented systems such as MSOT are user-friendly, special training of the clinical examiner is still needed. Hand-held optoacoustic probes are larger than normal ultrasound probes, and their use requires special consideration of laser safety. Interpretation of optoacoustic images at the moment requires understanding of the physics and computations involved, but clinical translation of optoacoustics will ultimately require specialized training that should not take longer than for other clinical imaging techniques.

8. Summary

The MSOT applications described herein demonstrate the broad capabilities of the technique to provide a multiscale assessment of the cardiovascular system, at all organization levels, in both the preclinical and clinical setting. Furthermore, in addition to the three spatial dimensions (3D) and time (4D), MSOT records the spectral signatures of scanned tissue, adding a fifth dimension (5D) to biomedical imaging applications. Specifically, in the spatial domain, MSOT enables the simultaneous extraction of information about many relevant length scales or orders of magnitude due to its higher depth-to-resolution ratio than pure optical methods. In the time domain, MSOT provides data acquisition at video-rates for the capture and analysis of dynamic phenomena occurring in the cardiovascular system. Finally, in the spectral domain, molecular signatures are overlaid onto anatomical and functional information to provide insights into tissue physiology, disease pathophysiology, and therapy monitoring.

In the cardiovascular system, MSOT can provide static anatomical information on the macro- and micro-vascular structures or lipid and collagen deposits with high composition-dependent contrast, as well as dynamic functional information about vascular wall dynamics and dimensions over the cardiac cycle with high temporal resolution. It allows label-free visualization of soft tissue perfusion, oxygen kinetics and metabolic activation over time and under different blood flow scenarios. When combined with appropriate exogenous optical contrast agents, MSOT can also provide complementary molecular information about inflammatory and other disease-specific processes.

The excellent capabilities of MSOT, such as for precise vascular imaging [126] and measurement of tissue oxygenation [27], may be further enhanced with other clinically-oriented optoacoustic technologies such as RSOM, which provide excellent visualization of microvasculature [87], thereby improving the precision of tissue imaging and the accuracy of medical diagnosis and therapy monitoring. Future development of compact, more sensitive ultrasound sensors, new illumination systems, and more precise reconstruction and spectral unmixing techniques will further foster the clinical translation of MSOT for cardiovascular and other applications. Although technically challenging, translation of MSOT from bench to bedside in the form of hybrid ultrasound-optoacoustic setups promises to address unanswered biological questions and meet urgent clinical needs.

Acknowledgements

We thank Dr. Christian Zakian, Dr. Murad Omar, Dr. Juan Aguirre, and Dr. A. Chapin Rodríguez for their invaluable help.

This project has received funding from the European Research Council (ERC) under the European Union's Horizon 2020 research and innovation program under grant agreement No 694968 (PREMSOT), from the Deutsche Forschungsgemeinschaft DFG with CRC 1123 (Z1) project Helmholtz Zentrum München under the funding program "Physician Scientists for Groundbreaking Projects".

References

[1] J.R. Lindner, Contrast ultrasound molecular imaging of inflammation in cardiovascular disease, Cardiovasc. Res. 84 (2) (2009) 182–189.
[2] K.S. Mehta, et al., Vascular applications of contrast-enhanced ultrasound imaging, J. Vasc. Surg. 66 (1) (2017) 266–274.
[3] A.F. Schinkel, M. Kaspar, D. Staub, Contrast-enhanced ultrasound: clinical applications in patients with atherosclerosis, Int. J. Cardiovasc. Imaging 32 (1) (2016) 35–48.
[4] K. Hawkins, J.S. Henry, R.A. Krasuski, Tissue harmonic imaging in echocardiography: better valve imaging, but at what cost? Echocardiography 25 (2) (2008) 119–123.
[5] M. Strachinaru, et al., Cardiac shear wave elastography using a clinical ultrasound system, Ultrasound Med. Biol. 43 (8) (2017) 1596–1606.
[6] R.J. Gibbons, et al., ACC/AHA 2002 guideline update for the management of patients with chronic stable angina–summary article: a report of the American College of Cardiology/American Heart Association Task Force on practice

guidelines (Committee on the Management of Patients With Chronic Stable Angina), J. Am. Coll. Cardiol. 41 (1) (2003) 159–168.
[7] G. Sianos, et al., Recanalisation of chronic total coronary occlusions: 2012 consensus document from the EuroCTO club, EuroIntervention 8 (1) (2012) 139–145.
[8] H. Ma, et al., Evaluation of motion artifact metrics for coronary CT angiography, Med. Phys. 45 (2) (2017) 687–702.
[9] W.W. Lee, et al., PET/MRI of inflammation in myocardial infarction, J. Am. Coll. Cardiol. 59 (2) (2012) 153–163.
[10] V. Rafailidis, et al., Imaging of the ulcerated carotid atherosclerotic plaque: a review of the literature, Insights Imaging 8 (2) (2017) 213–225.
[11] W.A. Zoghbi, Cardiovascular imaging: a glimpse into the future, Methodist Debakey Cardiovasc. J. 10 (3) (2014) 139–145.
[12] J.U. Doherty, et al., ACC/AATS/AHA/ASE/ASNC/HRS/SCAI/SCCT/SCMR/STS 2017 Appropriate Use Criteria for Multimodality Imaging in Valvular Heart Disease: A Report of the American College of Cardiology Appropriate Use Criteria Task Force, American Association for Thoracic Surgery, American Heart Association, American Society of Echocardiography, American Society of Nuclear Cardiology, Heart Rhythm Society, Society for Cardiovascular Angiography and Interventions, Society of Cardiovascular Computed Tomography, Society for Cardiovascular Magnetic Resonance, and Society of Thoracic Surgeons, J. Am. Coll. Cardiol. 70 (13) (2017) 1647–1672.
[13] C.S. Cina, C.M. Clase, B.R. Haynes, Refining the indications for carotid endarterectomy in patients with symptomatic carotid stenosis: a systematic review, J. Vasc. Surg. 30 (4) (1999) 606–617.
[14] H.M. Garcìa-Garcìa, et al., IVUS-based imaging modalities for tissue characterization: similarities and differences, Int. J. Cardiovasc. Imaging 27 (2011) 215–224.
[15] P. Kala, et al., OCT guidance during stent implantation in primary PCI: a randomized multicenter study with nine months of optical coherence tomography follow-up, Int. J. Cardiol. 250 (2018) 98–103.
[16] D. Bozhko, et al., Quantitative intravascular biological fluorescence-ultrasound imaging of coronary and peripheral arteries in vivo, Eur. Heart J. Cardiovasc. Imaging 18 (11) (2016) 1253–1261.
[17] F.A. Jaffer, et al., Two-dimensional intravascular near-infrared fluorescence molecular imaging of inflammation in atherosclerosis and stent-induced vascular injury, J. Am. Coll. Cardiol. 57 (2011) 2516–2526.
[18] M.A. Calfon, et al., Intravascular near-infrared fluorescence molecular imaging of atherosclerosis: toward coronary arterial visualization of biologically high-risk plaques, J. Biomed. Opt. 15 (2010) 011107.
[19] I.R. Efimov, V.P. Nikolski, G. Salama, Optical imaging of the heart, Circ. Res. 95 (1) (2004) 21–33.
[20] J.A. Scherschel, M. Rubart, Cardiovascular imaging using two-photon microscopy, Microsc. Microanal. 14 (6) (2008) 492–506.
[21] A. Arranz, et al., Fluorescent molecular tomography for in vivo imaging of mouse atherosclerosis, Methods Mol. Biol. 1339 (2015) 367–376.
[22] Z.-H. Yu, et al., Diagnosis of cardiovascular diseases based on diffuse optical tomography system, SPIE BiOS. 2008. International Society for Optics and Photonics, (2008).
[23] A. Rosencwaig, Photoacoustic spectroscopy of biological materials, Science 181 (4100) (1973) 657–658.
[24] A.A. Oraevsky, et al., Laser-based optoacoustic imaging in biological tissues, OE/LASE '94, (1994).
[25] R.A. Kruger, et al., Photoacoustic ultrasound (PAUS)–reconstruction tomography, Med. Phys. 22 (10) (1995) 1605–1609.
[26] A. Taruttis, V. Ntziachristos, Advances in real-time multispectral optoacoustic imaging and its applications, Nat. Photonics 9 (2015) 219–227.
[27] S. Tzoumas, et al., Eigenspectra optoacoustic tomography achieves quantitative blood oxygenation imaging deep in tissues, Nat. Commun. 7 (2016) 12121.
[28] C. Lutzweiler, D. Razansky, Optoacoustic imaging and tomography: reconstruction approaches and outstanding challenges in image performance and quantification, Sensors (Basel) 13 (2013) 7345–7384.
[29] G. Diot, et al., Multispectral optoacoustic tomography (MSOT) of human breast Cancer, Clin. Cancer Res. 23 (22) (2017) 6912–6922.
[30] A.A. Oraevsky, et al., Laser optoacoustic imaging of the breast: detection of cancer angiogenesis, BiOS '99 International Biomedical Optics Symposium (1999).
[31] I. Stoffels, et al., Metastatic status of sentinel lymph nodes in melanoma determined noninvasively with multispectral optoacoustic imaging, Sci. Transl. Med. 7 (317) (2015) p. 317ra199.
[32] F. Knieling, et al., Multispectral optoacoustic tomography for assessment of Crohn's disease activity, N. Engl. J. Med. 376 (13) (2017) 1292–1294.
[33] N. Beziere, et al., Optoacoustic imaging and staging of inflammation in a murine model of arthritis, Arthritis Rheumatol. 66 (8) (2014) 2071–2078.
[34] V. Gujrati, A. Mishra, V. Ntziachristos, Molecular imaging probes for multi-spectral optoacoustic tomography, Chem. Commun. (Camb.) 53 (34) (2017) 4653–4672.
[35] W. Li, X. Chen, Gold nanoparticles for photoacoustic imaging, Nanomedicine (Lond.) 10 (2) (2015) 299–320.
[36] N. Beziere, et al., Dynamic imaging of PEGylated indocyanine green (ICG) liposomes within the tumor microenvironment using multi-spectral optoacoustic tomography (MSOT), Biomaterials 37 (2015) 415–424.
[37] Y. Jiang, et al., Violacein as a genetically-controlled, enzymatically amplified and photobleaching-resistant chromophore for optoacoustic bacterial imaging, Sci. Rep. 5 (2015) 11048.
[38] L. Li, et al., Photoacoustic imaging of lacZ gene expression in vivo, J. Biomed. Opt. 12 (2) (2007) 020504.
[39] R.O. Esenaliev, et al., Continuous, noninvasive monitoring of total hemoglobin concentration by an optoacoustic technique, Appl. Opt. 43 (17) (2004) 3401–3407.
[40] M. Masthoff, et al., Use of multispectral optoacoustic tomography to diagnose vascular malformations, JAMA Dermatol. (2018).
[41] A.S. Bychkov, et al., On the use of an optoacoustic and laser ultrasonic imaging system for assessing peripheral intravenous access, Photoacoustics 5 (2017) 10–16.
[42] C. Zizola, P.C. Schulze, Metabolic and structural impairment of skeletal muscle in heart failure, Heart Fail. Rev. 18 (5) (2013) 623–630.
[43] C.M. Kramer, Skeletal muscle perfusion in peripheral arterial disease: a novel end point for cardiovascular imaging, JACC Cardiovasc. Imaging 1 (3) (2008) 351–353.
[44] L. Lin, et al., In vivo photoacoustic tomography of myoglobin oxygen saturation, J. Biomed. Opt. 21 (6) (2016) 61002.
[45] C. Zhang, et al., Label-free photoacoustic microscopy of myocardial sheet architecture, J. Biomed. Opt. 17 (2012) 060506.
[46] Y. Cao, et al., High-sensitivity intravascular photoacoustic imaging of lipid-laden plaque with a collinear catheter design, Sci. Rep. 6 (2016) 25236.
[47] A. Buehler, et al., Imaging of fatty tumors: appearance of subcutaneous lipomas in optoacoustic images, J. Biophotonics 10 (8) (2017) 983–989.
[48] P. Kruizinga, et al., Photoacoustic imaging of carotid artery atherosclerosis, J. Biomed. Opt. 19 (11) (2014) p. 110504–110504.
[49] S.K.V. Sekar, et al., Diffuse optical characterization of collagen absorption from 500 to 1700 nm, J. Biomed. Opt. 22 (1) (2017) p. 015006-015006.
[50] P. Wang, H.W. Wang, J.X. Cheng, Mapping lipid and collagen by multispectral photoacoustic imaging of chemical bond vibration, J. Biomed. Opt. 17 (9) (2012) 96010–96011.
[51] B.V. Shekhonin, et al., Distribution of type I, III, IV and V collagen in normal and atherosclerotic human arterial wall: immunomorphological characteristics, Coll. Relat. Res. 5 (4) (1985) 355–368.
[52] C.J. Ho, et al., Multifunctional photosensitizer-based contrast agents for photoacoustic imaging, Sci. Rep. 4 (2014) 5342.
[53] S. Friedrich, et al., Disturbed microcirculation in the hands of patients with systemic sclerosis detected by fluorescence optical imaging: a pilot study, Arthritis Res. Ther. 19 (1) (2017) 87.
[54] G.R. Cherrick, et al., Indocyanine green: observations on its physical properties, plasma decay, and hepatic extraction, J. Clin. Invest. 39 (4) (1960) 592–600.
[55] C. Vinegoni, et al., Indocyanine green enables near-infrared fluorescence imaging of lipid-rich, inflamed atherosclerotic plaques, Sci. Transl. Med. 3 (2011) p. 84ra45.
[56] J.W. Verjans, et al., Targeted near-infrared fluorescence imaging of atherosclerosis: clinical and intracoronary evaluation of Indocyanine Green, JACC Cardiovasc. Imaging 9 (9) (2016) 1087–1095.
[57] Y.W. Noh, et al., Enhancement of the photostability and retention time of indocyanine green in sentinel lymph node mapping by anionic polyelectrolytes, Biomaterials 32 (27) (2011) 6551–6557.
[58] T.P. Vacek, et al., Matrix metalloproteinases in atherosclerosis: role of nitric oxide, hydrogen sulfide, homocysteine, and polymorphisms, Vasc. Health Risk Manag. 11 (2015) 173–183.
[59] D. Razansky, et al., Multispectral optoacoustic tomography of matrix metalloproteinase activity in vulnerable human carotid plaques, Mol. Imaging Biol. 14 (3) (2011) 277–285.
[60] A. Taruttis, et al., Multispectral optoacoustic tomography of myocardial infarction, Photoacoustics 1 (1) (2013) 3–8.
[61] D. Myers Jret al., Selectins influence thrombosis in a mouse model of experimental deep venous thrombosis, J. Surg. Res. 108 (2) (2002) 212–221.
[62] S. Blankenberg, S. Barbaux, L. Tiret, Adhesion molecules and atherosclerosis, Atherosclerosis 170 (2) (2003) 191–203.
[63] T. Urakami, et al., In vivo distribution of liposome-encapsulated hemoglobin determined by positron emission tomography, Artif. Organs 33 (2) (2009) 164–168.
[64] C. Jung, et al., Intraperitoneal injection improves the uptake of nanoparticle-labeled high-density lipoprotein to atherosclerotic plaques compared with intravenous injection: a multimodal imaging study in ApoE knockout mice, Circ. Cardiovasc. Imaging 7 (2) (2014) 303–311.
[65] D. Danila, E. Johnson, P. Kee, CT imaging of myocardial scars with collagen-targeting gold nanoparticles, Nanomedicine 9 (7) (2013) 1067–1076.
[66] J.C. Stendahl, A.J. Sinusas, Nanoparticles for cardiovascular imaging and therapeutic delivery, part 1: compositions and features, J. Nucl. Med. 56 (10) (2015) 1469–1475.
[67] C.B. Collins, et al., Radiofrequency heating pathways for gold nanoparticles, Nanoscale 6 (15) (2014) 8459–8472.
[68] A. Taruttis, et al., Real-time imaging of cardiovascular dynamics and circulating gold nanorods with multispectral optoacoustic tomography, Opt. Express 18 (19) (2010) 19592–19602.
[69] S. Roberts, et al., Calcium sensor for photoacoustic imaging, J. Am. Chem. Soc. 140 (8) (2017) 2718–2721.

[70] A. Mishra, et al., Near-infrared photoacoustic imaging probe responsive to calcium, Anal. Chem. 88 (22) (2016) 10785–10789.
[71] G.S. Filonov, et al., Deep-tissue photoacoustic tomography of genetically encoded iRFP probe, Angew. Chem. Int. Ed. Engl. 51 (6) (2012) 1448–1451.
[72] D. Razansky, et al., Multispectral opto-acoustic tomography of deep-seated fluorescent proteins in vivo, Nat. Photonics 3 (7) (2009) 412–417.
[73] C. Qin, et al., Tyrosinase as a multifunctional reporter gene for Photoacoustic/MRI/PET triple modality molecular imaging, Sci. Rep. 3 (2013) 1490.
[74] J. Yao, et al., Multi-scale photoacoustic tomography using reversibly switchable bacterial phytochrome as a near-infrared photochromic probe, Nat. Methods 13 (1) (2016) 67–73.
[75] J. Akerboom, et al., Optimization of a GCaMP calcium indicator for neural activity imaging, J. Neurosci. 32 (40) (2012) 13819–13840.
[76] X.L. Deán-Ben, et al., Functional optoacoustic neuro-tomography for scalable whole-brain monitoring of calcium indicators, Light Sci. Appl. 5 (12) (2016) e16201.
[77] A. Taruttis, G.M. van Dam, V. Ntziachristos, Mesoscopic and macroscopic optoacoustic imaging of cancer, Cancer Res. 75 (8) (2015) 1548–1559.
[78] J. Reber, et al., Non-invasive measurement of brown fat metabolism based on optoacoustic imaging of hemoglobin gradients, Cell Metab. 27 (3) (2018) 689–701 e4.
[79] Y. Li, et al., Secretin-activated brown fat mediates prandial thermogenesis to induce satiation, Cell 175 (6) (2018) 1561–1574 e12.
[80] A. Dima, N.C. Burton, V. Ntziachristos, Multispectral optoacoustic tomography at 64, 128, and 256 channels, J. Biomed. Opt. 19 (2014) 036021.
[81] A. Taruttis, et al., Optoacoustic imaging of human vasculature: feasibility by using a handheld probe, Radiology (2016) 152160.
[82] E. Herzog, et al., Optical imaging of cancer heterogeneity with multispectral optoacoustic tomography, Radiology 263 (2012) 461–468.
[83] N.C. Burton, et al., Multispectral opto-acoustic tomography (MSOT) of the brain and glioblastoma characterization, Neuroimage 65 (2013) 522–528.
[84] S. Morscher, et al., Semi-quantitative Multispectral Optoacoustic Tomography (MSOT) for volumetric PK imaging of gastric emptying, Photoacoustics 2 (2014) 103–110.
[85] L. Vionnet, et al., 24-MHz scanner for optoacoustic imaging of skin and burn, IEEE Trans. Med. Imaging 33 (2) (2014) 535–545.
[86] M. Omar, et al., Pushing the optical imaging limits of cancer with multi-frequency-band raster-scan optoacoustic mesoscopy (RSOM), Neoplasia 17 (2) (2015) 208–214.
[87] J. Aguirre, et al., Precision assessment of label-free psoriasis biomarkers with ultra-broadband optoacoustic mesoscopy, Nat. Biomed. Eng. 1 (2017) 0068.
[88] T.F. Antonios, et al., Structural skin capillary rarefaction in essential hypertension, Hypertension 33 (1999) 998–1001.
[89] T.F. Antonios, et al., Rarefaction of skin capillaries in patients with anginal chest pain and normal coronary arteriograms, Eur. Heart J. 22 (2001) 1144–1148.
[90] A. Uliasz, M. Lebwohl, Cutaneous manifestations of cardiovascular diseases, Clin. Dermatol. 26 (2008) 243–254.
[91] J. Aguirre, et al., Broadband mesoscopic optoacoustic tomography reveals skin layers, Opt. Lett. 39 (2014) 6297–6300.
[92] M. Schwarz, et al., Motion correction in optoacoustic mesoscopy, Sci. Rep. 7 (1) (2017) 10386.
[93] K. Yahagi, et al., Pathophysiology of native coronary, vein graft, and in-stent atherosclerosis, Nat. Rev. Cardiol. 13 (2) (2016) 79–98.
[94] J. Pu, et al., Insights into echo-attenuated plaques, echolucent plaques, and plaques with spotty calcification: novel findings from comparisons among intravascular ultrasound, near-infrared spectroscopy, and pathological histology in 2,294 human coronary artery segments, J. Am. Coll. Cardiol. 63 (21) (2014) 2220–2233.
[95] G.W. Stone, et al., A prospective natural-history study of coronary atherosclerosis, N. Engl. J. Med. 364 (3) (2011) 226–235.
[96] M. Wu, et al., Impact of device geometry on the imaging characteristics of an intravascular photoacoustic catheter, Appl. Opt. 53 (34) (2014) 8131–8139.
[97] J. Yao, L.V. Wang, Photoacoustic microscopy, Laser Photon. Rev. 7 (5) (2013).
[98] P. Helm, et al., Measuring and mapping cardiac fiber and laminar architecture using diffusion tensor MR imaging, Ann. N. Y. Acad. Sci. 1047 (2005) 296–307.
[99] S.B. Kanatous, P.P.A. Mammen, Regulation of myoglobin expression, J. Exp. Biol. 213 (16) (2010) 2741–2747.
[100] Q. Chen, et al., Label-free photoacoustic imaging of the cardio-cerebrovascular development in the embryonic zebrafish, Biomed. Opt. Express 8 (4) (2017) 2359–2367.
[101] M. Seeger, et al., Multimodal optoacoustic and multiphoton microscopy of human carotid atheroma, Photoacoustics 4 (3) (2016) 102–111.
[102] G.J. Tserevelakis, et al., Hybrid multiphoton and optoacoustic microscope, Opt. Lett. 39 (2014) 1819–1822.
[103] R. Virmani, Atherosclerotic plaque progression and vulnerability to rupture: angiogenesis as a source of intraplaque hemorrhage, Arterioscler. Thromb. Vasc. Biol. 25 (2005) 2054–2061.
[104] G. Asciutto, et al., Low elastin content of carotid plaques is associated with increased risk of ipsilateral stroke, PLoS One 10 (3) (2015) e0121086.
[105] M.D. Rekhter, Collagen synthesis in atherosclerosis: too much and not enough, Cardiovasc. Res. 41 (1999) 376–384.
[106] D. Soliman, et al., Combining microscopy with mesoscopy using optical and optoacoustic label-free modes, Sci. Rep. (2015) 1–9.
[107] J.M. Frank, et al., Microcirculation research, angiogenesis, and microsurgery, Microsurgery 15 (6) (1994) 399–404.
[108] S. Attanasio, J. Snell, Therapeutic angiogenesis in the management of critical limb ischemia: current concepts and review, Cardiol. Rev. 17 (3) (2009) 115–120.
[109] C. Camaré, et al., Angiogenesis in the atherosclerotic plaque, Redox Biol. 12 (2017) 18–34.
[110] M.J. Fowler, Microvascular and macrovascular complications of diabetes, Clin. Diabetes 29 (3) (2011) 116–122.
[111] R.Z.L. Humar, E. Battegay, Angiogenesis and hypertension: an update, J. Hum. Hypertens. 23 (12) (2009) 773–782.
[112] V. Ntziachristos, D. Razansky, Molecular imaging by means of multispectral optoacoustic tomography (MSOT), Chem. Rev. 110 (2010) 2783–2794.
[113] A.J. Brown, et al., Role of biomechanical forces in the natural history of coronary atherosclerosis, Nat. Rev. Cardiol. 13 (4) (2016) 210–220.
[114] Y. Zhao, et al., Mechanical evaluation of lipid accumulation in atherosclerotic tissues by photoacoustic viscoelasticity imaging, Opt. Lett. 41 (19) (2016) 4522–4525.
[115] L. Cardoso, S. Weinbaum, Changing views of the biomechanics of vulnerable plaque rupture, a review, Ann. Biomed. Eng. 42 (2) (2014) 415–431.
[116] G. Baltgaile, Arterial wall dynamics, Perspect. Med. 1 (2012) 146–151.
[117] M. Zaromytidou, et al., Intravascular hemodynamics and coronary artery disease: new insights and clinical implications, Hellenic J. Cardiol. 57 (6) (2016) 389–400.
[118] C. Yeh, et al., Photoacoustic microscopy of blood pulse wave, J. Biomed. Opt. 17 (7) (2012).
[119] N. Di Lascio, et al., Non-invasive assessment of pulse wave velocity in mice by means of ultrasound images, Atherosclerosis 237 (1) (2014) 31–37.
[120] Collaboration, T.R.V.f.A.S, Determinants of pulse wave velocity in healthy people and in the presence of cardiovascular risk factors: 'establishing normal and reference values', Eur. Heart J. 31 (19) (2010) 2338–2350.
[121] A. Taruttis, et al., Motion clustering for deblurring multispectral optoacoustic tomography images of the mouse heart, J. Biomed. Opt. 17 (1) (2012) 016009.
[122] M.T. Berninger, et al., Detection of intramyocardially injected DiR-labeled mesenchymal stem cells by optical and optoacoustic tomography, Photoacoustics 6 (2017) 37–47.
[123] X.L. Dean-Ben, S.J. Ford, D. Razansky, High-frame rate four dimensional optoacoustic tomography enables visualization of cardiovascular dynamics and mouse heart perfusion, Sci. Rep. 5 (2015) 10133.
[124] P. Slomka, et al., The role of PET quantification in cardiovascular imaging, Clin. Transl. Imaging 2 (4) (2014) 343–358.
[125] E. Lin, A. Alessio, What are the basic concepts of temporal, contrast, and spatial resolution in cardiac CT? J. Cardiovasc. Comput. Tomogr. 3 (6) (2009) 403–408.
[126] A. Karlas, et al., Flow-mediated dilatation test using optoacoustic imaging: a proof-of-concept, Biomed. Opt. Express 8 (7) (2017) 3395–3403.
[127] A. Dima, V. Ntziachristos, Non-invasive carotid imaging using optoacoustic tomography, Opt. Express 20 (2012) 25044–25057.
[128] America., T.L.I.o, American National Standards for the Safe Use of Lasers, ANSI Z136.1, 2000.
[129] E. Ohmae, et al., Sensitivity correction for the influence of the fat layer on muscle oxygenation and estimation of fat thickness by time-resolved spectroscopy, J. Biomed. Opt. 19 (6) (2014) 067005.
[130] B. Wang, et al., Intravascular photoacoustic imaging of lipid in atherosclerotic plaques in the presence of luminal blood, Opt. Lett. 37 (7) (2012) 1244–1246.
[131] J. Zhang, et al., Characterization of lipid-rich aortic plaques by intravascular photoacoustic tomography: ex vivo and in vivo validation in a rabbit atherosclerosis model with histologic correlation, J. Am. Coll. Cardiol. 64 (4) (2014) 385–390.
[132] G. Diot, A. Dima, V. Ntziachristos, Multispectral opto-acoustic tomography of exercised muscle oxygenation, Opt. Lett. 40 (2015) 1496–1499.
[133] C.V. Bourantas, et al., Hybrid intravascular imaging: recent advances, technical considerations, and current applications in the study of plaque pathophysiology, Eur. Heart J. 38 (6) (2017) 400–412.
[134] O. Manfrini, et al., Sources of error and interpretation of plaque morphology by optical coherence tomography, Am. J. Cardiol. 98 (2) (2006) 156–159.
[135] C.M. Gardner, et al., Detection of lipid core coronary plaques in autopsy specimens with a novel catheter-based near-infrared spectroscopy system, JACC Cardiovasc. Imaging 1 (5) (2008) 638–648.
[136] J. Bec, et al., In-vivo Validation of Fluorescence Lifetime Imaging (FLIm) of Coronary Arteries in Swine. In SPIE BiOS, International Society for Optics and Photonics, 2017.
[137] M. Abran, et al., Validating a bimodal intravascular ultrasound (IVUS) and near-infrared fluorescence (NIRF) catheter for atherosclerotic plaque detection in rabbits, Biomed. Opt. Express 6 (10) (2015) 3989–3999.
[138] J. Chen, et al., In vivo imaging of proteolytic activity in atherosclerosis, Circulation 105 (23) (2002) 2766–2771.
[139] R.Y. Khamis, et al., Near infrared fluorescence (NIRF) molecular imaging of oxidized LDL with an autoantibody in experimental atherosclerosis, Sci. Rep. 6 (2016) 21785.
[140] M. Abran, et al., Development of a photoacoustic, ultrasound and fluorescence imaging catheter for the study of atherosclerotic plaque, IEEE Trans. Biomed. Circuits Syst. 8 (5) (2014) 696–703.
[141] D. VanderLaan, et al., Real-time intravascular ultrasound and photoacoustic imaging, IEEE Trans. Ultrason. Ferroelectr. Freq. Control 64 (1) (2017) 141–149.
[142] S.J. Mathews, et al., All-optical dual photoacoustic and optical coherence tomography intravascular probe, Photoacoustics 11 (2018) 65–70.
[143] Y. Cao, et al., High-sensitivity intravascular photoacoustic imaging of lipid–laden

plaque with a collinear catheter design, Sci. Rep. (2016).
[144] J. Hui, et al., Real-time intravascular photoacoustic-ultrasound imaging of lipid-laden plaque in human coronary artery at 16 frames per second, Sci. Rep. 7 (1) (2017) 1417.

Angelos Karlas studied Medicine (M.D.) and Electrical and Computer Engineering (Dipl.-Ing.) at the Aristotle University of Thessaloniki, Greece. He holds a Master of Science in Medical Informatics (M.Sc.) from the same university and a Master of Research (M.Res.) in Medical Robotics and Image-Guided Intervention from Imperial College London, UK. He currently works as clinical resident at the Department for Vascular and Endovascular Surgery of the Rechts der Isar University Hospital in Munich, Germany. He holds the position of the Clinical Translation Manager at the Institute for Biological and Medical Imaging of the Helmholtz Center Munich and the Technical University of Munich, Germany, while pursuing his Ph.D. (Dr.rer.nat.) in Experimental Medicine at the same university. He also serves as the Group Leader of the Clinical Translation Group at the Institute for Biological and Medical Imaging of the Technical University of Munich, Germany. His research interests are in the areas of innovative vascular imaging and image-guided vascular interventions.

Professor Vasilis Ntziachristos received his PhD in electrical engineering from the University of Pennsylvania, USA, followed by a postdoctoral position at the Center for Molecular Imaging Research at Harvard Medical School. Afterwards, he became an Instructor and following an Assistant Professor and Director at the Laboratory for Bio-Optics and Molecular Imaging at Harvard University and Massachusetts General Hospital, Boston, USA. Currently, he is the Director of the Institute for Biological and Medical Imaging at the Helmholtz Zentrum in Munich, Germany, as well as a Professor of Electrical Engineering, Professor of Medicine and Chair for Biological Imaging at the Technical University Munich. His work focuses on novel innovative optical and optoacoustic imaging modalities for studying biological processes and diseases as well as the translation of these findings into the clinic.